Journal of Magnetic Resonance 305 (2019) 1–4

Contents lists available at ScienceDirect

Journal of Magnetic Resonance

journal homepage: www.elsevier.com/locate/jmr

Correcting for magnetic field drift in magic-angle spinning NMR datasets

Eszter E. Najbauer, Loren B. Andreas *

Max Planck Institute for Biophysical Chemistry, Am Faßberg 11, D-37077 Göttingen, Germany

ARTICLE INFO

Article history:
Received 6 March 2019
Revised 7 May 2019
Accepted 15 May 2019
Available online 16 May 2019

Keywords:
Magnetic field drift
Proton detection
Magic-angle spinning
Membrane protein

ABSTRACT

Magnetic field drift during magic angle spinning (MAS) NMR measurements is detrimental to the spectra, causing broadening of lines and distortion of lineshapes, especially in high-quality samples with linewidths of less than 0.1 ppm. We report that a simple linear correction for magnet drift can be used to improve the quality of proton detected MAS NMR measurements. Despite the fact that the magnetic field of superconducting magnets changes in a non-linear fashion, we find that when data acquisition is sufficiently short, a linear correction is a good approximation to the actual field drift. We used a script written in the C programming language for linear drift correction of multidimensional datasets (2D, 3D, 4D), which can be executed directly from Bruker Topspin. A second script allows datasets to be subdivided into arbitrarily short measurements, individually corrected, and concatenated before processing.

1. Introduction

Drift in the main magnetic field in magnetic resonance techniques is a well-known issue. If not corrected for, the drift of the B_0 magnetic field results in broadening of spectral peaks and distortion of lineshapes. In magnetic resonance imaging (MRI), using spectral registration, each spectral average is fit to a reference scan in the time domain by adjusting both frequency and phase terms [1]. In solution NMR spectroscopy, the issue is usually solved by correcting the magnetic field while the measurement is recorded. This field lock is typically implemented by tracking the field drift by detecting deuterium and constantly adjusting the main field with the use of room temperature electromagnets [2,3].

In magic angle spinning (MAS) NMR measurements, this solution can be impractical, due to the small sample volume, which results in low sensitivity of deuterium and an unstable lock. Additionally, many probes built for proton detected MAS NMR do not have a deuterium channel. An alternative approach for carbon detected spectra is to use the proton channel for a lock [4]. External locks can also be used to track the main field. In this case, a small sample (e.g. containing deuterium oxide in solution) is placed close to the MAS rotor in its own dedicated detection coil [5]. Such external lock systems are available from instrument manufacturers, but they do not entirely remove drift, since they are not detecting the field at the sample, and in addition, they are often not temperature controlled, resulting in a long equilibration time before the temperature sensitive D_2O sample can be used. The result is that MAS NMR data is often acquired while the main field drifts. Even adjusting the linear drift compensation of the spectrometer, we often observe drift of up to 0.075 ppm after a 24 h measurement. For ^{13}C-detected data, this is usually insignificant, since linewidths are generally greater than 0.3 ppm. However, proton-detected spectra of deuterated microcrystals can have linewidths below 0.05 ppm [6,7], and even the less ideal preparations of membrane proteins can have linewidths of around 0.1 ppm [8].

In solution NMR, the lock is also important in order to maintain good water suppression. This is because the typically used water suppression schemes, such as presaturation methods [9–11] and WATERGATE [12,13] are highly dependent on the carrier frequency. With a small drift, the water suppression can be severely compromised. This is not the case in cross polarization-based proton detected MAS NMR, where the water is suppressed by relatively strong saturation pulses [14–16]. It is therefore possible to correct for large drift in the field, provided the drift is known. Alternatively, the drift may be assumed to be linear if the acquisition time is made sufficiently short such that a linear correction is a good approximation of the actual drift.

2. Linear phase correction of the FID

We apply two principles to acquire the best resolution possible under conditions of a slow field drift. First, we acquire data in short blocks of about 24 h, or even shorter, such that the drift over this time will be approximately linear. Longer acquisitions can be divided into 24–36 h acquisitions by use of reduced phase cycles and non-uniform sampling. Next, we correct the data in the time domain assuming linear drift occurred during the measurement.

* Corresponding author.
E-mail address: land@nmr.mpibpc.mpg.de (L.B. Andreas).

https://doi.org/10.1016/j.jmr.2019.05.005
1090-7807/

This drift is determined from a one dimensional (1D) spectrum with a sensitive and narrow line. Correction of a signal with frequency ν by a frequency offset ν_0 in the time domain is simply a linear ramp in the phase, according to the well-known Fourier relation [17,18]. Applying a linear phase ramp of $2\pi\nu_0$ to an FID of $S(t) = S_0 \cdot \exp(i2\pi\nu t_{aq})$, we obtain the expected frequency shift of ν_0, which can be seen in either the time domain, or in the frequency domain after Fourier transformation:

$$S(t) \cdot \exp(i2\pi\nu_0 t_{aq})) = S_0 \cdot \exp(i2\pi\nu t_{aq}) \cdot \exp(i2\pi\nu_0 t_{aq})) = S_0 \cdot \exp(i2\pi(\nu+\nu_0)t_{aq}) \overset{FT}{\rightarrow} S(\nu+\nu_0) \quad (1)$$

For multidimensional data, the correction is made across each dimension, keeping track of multiple time values: the actual point in time when the data was acquired, as well as the evolution time in each indirect dimension. The actual time determines the frequency correction needed, while the indirect evolution determines the location on the linear ramp. For best results, all the phases for a complex point should be acquired before moving to the next point, such that all phases are acquired at nearly the same magnetic field. In practice, we have found that the drift is small enough that the data can be acquired as planes, and it can be assumed that the full plane was acquired at a single magnetic field.

For correction of a complex point for 2D spectra, the correction is extended as follows. In a 2D spectrum, one complex point comprises 4 FIDs: rr (real in both indirect and direct dimensions), ri (real in indirect, imaginary in direct dimension), ir (imaginary in indirect, real in direct dimension), and ii (imaginary in both dimensions).

The phase correction to be applied to any complex point consisting of 4 FIDs in the direct dimension is:

$$\phi_{dir} = \left(f_{start} + i\frac{f_{end} - f_{start}}{n}\right) t_{dir} * 2\pi \quad (2)$$

where ϕ_{dir} is the phase correction needed for correction the direct dimension, f_{start} and f_{end} are the required frequency shifts (measured on reference 1D spectra) at the beginning and end of recording the given spectrum, n is the total number of complex points in the spectrum, i is the index of the complex point, and $t_{dir} = j * dw_{dir}$ is the acquisition time up to that point in the direct dimension, where j is the corrected point's index within the FID, and dw_{dir} is the dwell time in the direct dimension. The phase correction for the direct dimension is done looping through the 4 FIDs belonging to the complex point.

After correction of drift in the direct dimension, the FIDs are: rr_c, ri_c, ir_c, ii_c:

$$rr_c = \cos\phi_{dir} * rr - \sin\phi_{dir} * ri \quad (3)$$

$$ri_c = \sin\phi_{dir} * rr + \cos\phi_{dir} * ri \quad (4)$$

$$ir_c = \cos\phi_{dir} * ir - \sin\phi_{dir} * ii \quad (5)$$

$$ii_c = \sin\phi_{dir} * ir + \cos\phi_{dir} * ii \quad (6)$$

The correction of the indirect dimension is done similarly. The phase is calculated:

$$\phi_{id} = \left(f_{start} + i\frac{f_{end} - f_{start}}{n}\right) t_{id} * 2\pi * \frac{\gamma_{id}}{\gamma_{dir}} \quad (7)$$

where all notations previously defined remain the same, γ_{dir} and γ_{id} are the gyromagnetic ratios of the detected nucleus and the nucleus in the indirect dimension, respectively, and $t_{id} = dw_{id} * i$, with dw_{id} being the dwell time in the indirect dimension.

The FIDs also corrected for drift in the indirect dimension thus are:

$$rr_{cc} = \cos\phi_{id} * rr_c - \sin\phi_{id} * ri_c \quad (8)$$

$$ri_{cc} = \sin\phi_{id} * rr_c + \cos\phi_{id} * ri_c \quad (9)$$

$$ir_{cc} = \cos\phi_{id} * ir_c - \sin\phi_{id} * ii_c \quad (10)$$

$$ii_{cc} = \sin\phi_{id} * ir_c + \cos\phi_{id} * ii_c \quad (11)$$

This principle can be extended to an arbitrary number of dimensions. The script used for drift correction of phase-sensitive data up to 4 dimensions is available in the Supplemental Information.

3. Application of drift correction

While datasets may contain no drift at all, we have found that occasionally, data would need to be thrown away if correction were not used. For example, the rate of drift is different and unpredictable for several days after filling helium. Also, when recording data over the course of several weeks, the linear drift compensation of the magnet may not be sufficient, and drifts of up to hundreds of proton Hz are not uncommon. The linear component of the field drift during measurements can be determined by recording a 1D spectrum directly before and after the experiment. For biological samples, the proton 1D spectrum typically contains sufficient water, lipids, or other narrow signals with high intensity that can be used to precisely determine the drift.

We demonstrate drift correction using 2D, 3D and 4D spectra recorded on a sample of the human voltage-dependent anion channel (VDAC) in lipid bilayers [19–21]. All spectra were measured using a 1.3 mm HCN probe on a Bruker Avance III 800 MHz narrow bore spectrometer at 55 kHz MAS.

A 2D spectrum was recorded in 96 scans per point over an 8 h period during which the linear drift compensation (31 proton Hz/h) was turned off (Fig. 1). The 3D spectrum, (H)CONH, of Figs. 2 and 3, was measured over 12 h following a reset of the Z0 shim coil, which is needed on our 800 MHz instrument every ~6 months. As an example of a 4D spectrum, we recorded the H

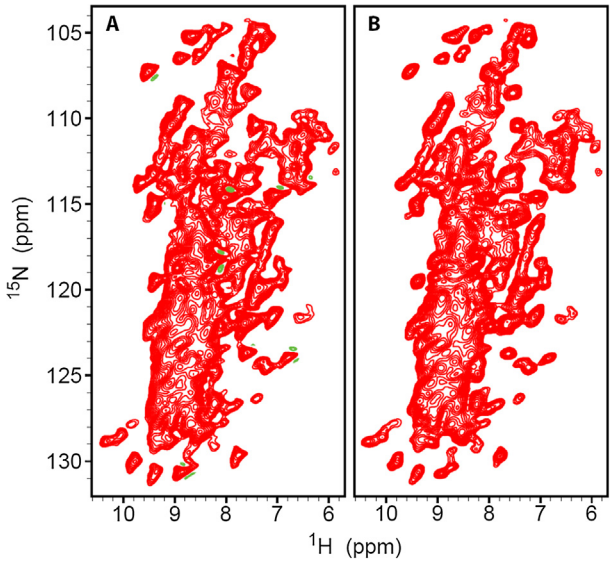

Fig. 1. 2D (H)NH spectrum acquired without compensation for drift in the magnetic field (A). Several peaks are distorted and show "butterfly" peak shapes characteristic of a large drift (294 Hz over the measurement). After applying linear drift correction to the recorded data (B), the peak distortion disappears and the expected round peak shape is restored.

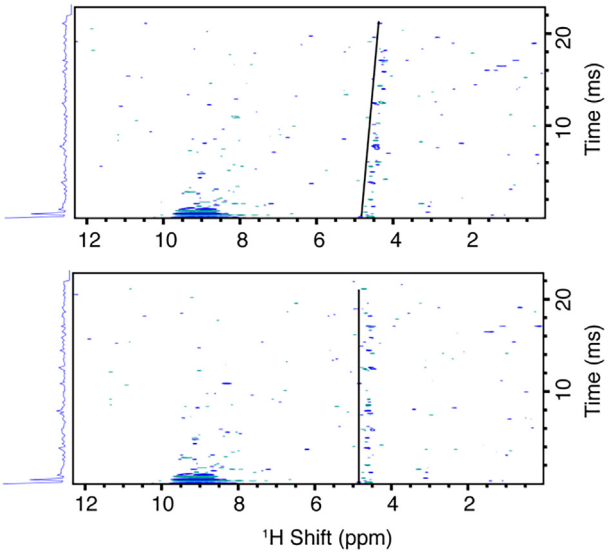

Fig. 2. Drift during a 12 h acquisition of the 3D spectrum (H)CONH. The spectrum was Fourier transformed in the direct dimension, and shows the drift over the total acquisition on the time axis. The acquisition followed a reset of the room temperature Z0 shim coil when the drift rate is unpredictable. The residual water shows that the drift is linear to a good approximation. The total drift during the acquisition was 304 Hz (0.38 ppm) as determined from proton 1D spectra acquired directly before and after the measurement.

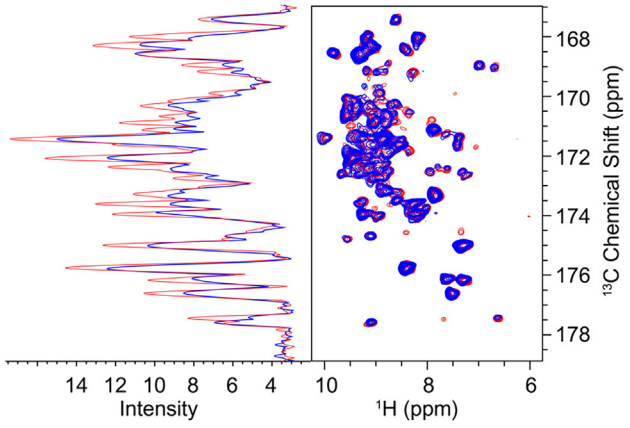

Fig. 3. Comparison of the corrected (red) and uncorrected (blue) 3D (H)CONH spectrum of Fig. 2. The CO-H projection of the full 3D dataset is shown, together with a double projection onto the ^{13}C axis to show the improvement in sensitivity after correction.

(H)CANH sequence, modified from the out-and-back variants in Ref. [22]. The spectrum was recorded in one-day blocks of 2 scans per point by applying 3.55% non-uniform sampling. In total, 19 blocks were recorded over 3 weeks and averaged either before or after drift correction (Fig. 4). Although the linear drift compensation was active during the whole measurement, the magnet drifted within a range of ~350 Hz. The multi-dimensional decomposition (MDD) algorithm [23] in Topsin version 3.5 was used for reconstruction.

The drift correction for each spectrum was performed in Topspin using the script provided in the SI. Since the script is based on the C programming language, it can be easily modified for other data acquisition and processing environments by adapting the Bruker-specific AU commands used to read acquisition parameters. The runtime of the script is less than a second on typical personal computers, even for 4D data with >5000 complex points.

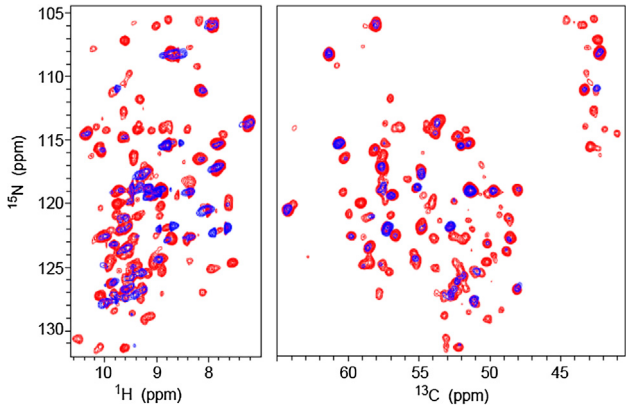

Fig. 4. Overlay of ^{1}H-^{15}N and the ^{13}C-^{15}N projections of a 4D H(H)CANH spectrum recorded over 3 weeks with (red) and without (blue) correcting the field drift (maximum 350 Hz during the time of acquisition). The two spectra are contoured at the same intensity levels. Reduced intensity is clearly visible in the uncorrected projections. The HN projection also displays elongated peak shapes in the ^{1}H dimension, as proton resonances are narrow in ppm, thus the field drift also has a greater effect on the peak shapes of this dimension. 75 ms of longitudinal ^{1}H-^{1}H mixing was used.

The uncorrected 2D (H)NH spectrum is characterized by distorted triangular ("butterfly") peak shapes. Essentially, one side of the line is artificially narrowed, while the other side is artificially broadened during the drift (Fig. 1A). Correction of the drift eliminates peak shape distortions and restores the expected round peak shapes (Fig. 1B).

In Fig. 2, the drift during the 3D dataset is shown after transformation of the direct dimension. The drift over the duration of the acquisition is seen on the residual t_1 noise from water (top) and the improvement is seen after correction (bottom). In the 3D and 4D spectra, the effect of the drift in the processed spectra is most apparent in the reduced peak intensities (Figs. 3 and 4), as well as in elongated peak shapes in the proton dimension (Fig. 4). In the 3D spectrum, drift correction resulted in a 20 percent improvement in peak height.

4. Conclusions

We present a simple method to correct for drift occurring while recording MAS NMR spectra in the absence of a lock. We demonstrate that the detrimental effect of a significant field drift can be minimized if the data is recorded in short blocks and, after acquisition, a linear phase ramp calculated from the drift during each experiment is applied to each spectrum across all dimensions. We show that drift correction leads to a significant increase in peak intensity and improved peak shapes. The script provided in the SI is capable of correcting linear drift in all dimensions of a 2D, a 3D or a 4D spectrum recorded as planes, points or using non-uniform sampling. A second script is provided for the case that a dataset with minimum phase cycle exceeds the time over which linear compensation can be used. In this case, the dataset can be subdivided and later concatenated. Details are provided in the header of the script.

Declaration of Competing Interest

None.

Acknowledgments

We thank Karin Giller and Stefan Becker for preparation of the VDAC sample. We thank Wolfgang Bermel for his help in under-

standing the data structure of the binary file containing time domain data, the 'ser' file, stored by Bruker Topspin, and initial direction in implementing the script.

This research was supported by the Deutsche Forschungsgemeinschaft through grants SFB803 INST 186/794-3 project A04 and the Emmy Noether program grant AN1316/1-1.

Appendix A. Supplementary material

Supplementary data to this article can be found online at https://doi.org/10.1016/j.jmr.2019.05.005.

References

[1] J. Near, R. Edden, C.J. Evans, R. Paquin, A. Harris, P. Jezzard, Frequency and phase drift correction of magnetic resonance spectroscopy data by spectral registration in the time domain, Magn. Reson. Med. 73 (2015) 44–50, https://doi.org/10.1002/mrm.25094.
[2] E.B. Baker, L.W. Burd, High stability nuclear magnetic resonance spectrograph, Rev. Sci. Instrum. 28 (1957) 313–321, https://doi.org/10.1063/1.1715873.
[3] D.C. Hofer, V.N. Kahwaty, C.R. Valentino, NMR field frequency lock system, US Pat. # 4,110,681, 1978-08-29.
[4] T. Maly, J. Bryant, D. Ruben, R.G. Griffin, A field-sweep/field-lock system for superconducting magnets–Application to high-field EPR, J. Magn. Reson. 183 (2006) 303–307, https://doi.org/10.1016/j.jmr.2006.09.012.
[5] E.K. Paulson, K.W. Zilm, External field-frequency lock probe for high resolution solid state NMR, Rev. Sci. Instrum. 76 (2005), https://doi.org/10.1063/1.1841972.
[6] J.R. Lewandowski, J.N. Dumez, U. Akbey, S. Lange, L. Emsley, H. Oschkinat, Enhanced resolution and coherence lifetimes in the solid-state NMR spectroscopy of perdeuterated proteins under ultrafast magic-angle spinning, J. Phys. Chem. Lett. 2 (2011) 2205–2211, https://doi.org/10.1021/jz200844n.
[7] V. Agarwal, S. Penzel, K. Szekely, R. Cadalbert, E. Testori, A. Oss, J. Past, A. Samoson, M. Ernst, A. Bockmann, B.H. Meier, De novo 3D structure determination from sub-milligram protein samples by solid-state 100 kHz MAS NMR spectroscopy, Angew. Chem. Int. Ed. Engl. 53 (2014) 12253–12256, https://doi.org/10.1002/anie.201405730.
[8] N.A. Lakomek, L. Frey, S. Bibow, A. Bockmann, R. Riek, B.H. Meier, Proton-detected NMR spectroscopy of nanodisc-embedded membrane proteins: MAS solid-state vs solution-state methods, J. Phys. Chem. B 121 (2017) 7671–7680, https://doi.org/10.1021/acs.jpcb.7b06944.
[9] D. Neuhaus, I.M. Ismail, C.W. Chung, "FLIPSY" - A new solvent-suppression sequence for nonexchanging solutes offering improved integral accuracy relative to 1D NOESY, J. Magn. Reson. Ser. A 118 (1996) 256–263, https://doi.org/10.1006/jmra.1996.0034.
[10] A.J. Simpson, S.A. Brown, Purge NMR: effective and easy solvent suppression, J. Magn. Reson. 175 (2005) 340–346, https://doi.org/10.1016/j.jmr.2005.05.008.
[11] H.P. Mo, D. Raftery, Pre-SAT180, a simple and effective method for residual water suppression, J. Magn. Reson. 190 (2008) 1–6, https://doi.org/10.1016/j.jmr.2007.09.016.
[12] M. Piotto, V. Saudek, V. Sklenar, Gradient-tailored excitation for single-quantum NMR spectroscopy of aqueous solutions, J. Biomol. NMR 2 (1992) 661–665, https://doi.org/10.1007/BF02192855.
[13] V. Sklenar, M. Piotto, R. Leppik, V. Saudek, Gradient-tailored water suppression for H-1-N-15 Hsqc experiments optimized to retain full sensitivity, J. Magn. Reson. Ser. A 102 (1993) 241–245, https://doi.org/10.1006/jmra.1993.1098.
[14] D.H. Zhou, C.M. Rienstra, High-performance solvent suppression for proton detected solid-state NMR, J. Magn. Reson. 192 (2008) 167–172, https://doi.org/10.1016/j.jmr.2008.01.012.
[15] E. Barbet-Massin, A.J. Pell, J.S. Retel, L.B. Andreas, K. Jaudzems, W.T. Franks, A.J. Nieuwkoop, M. Hiller, V. Higman, P. Guerry, A. Bertarello, M.J. Knight, M. Felletti, T. Le Marchand, S. Kotelovica, I. Akopjana, K. Tars, M. Stoppini, V. Bellotti, M. Bolognesi, S. Ricagno, J.J. Chou, R.G. Griffin, H. Oschkinat, A. Lesage, L. Emsley, T. Herrmann, G. Pintacuda, Rapid proton-detected NMR assignment for proteins with fast magic angle spinning, J. Am. Chem. Soc. 136 (2014) 12489–12497, https://doi.org/10.1021/ja507382j.
[16] P. Fricke, V. Chevelkov, M. Zinke, K. Giller, S. Becker, A. Lange, Backbone assignment of perdeuterated proteins by solid-state NMR using proton detection and ultrafast magic-angle spinning, Nat. Protocol 12 (2017) 764–782, https://doi.org/10.1038/nprot.2016.190.
[17] J.B.J. Fourier, Théorie analytique de la chaleur, Chez Firmin Didot, Père et Fils, Paris, 1822.
[18] J.B.J. Fourier, The Analytical Theory of Heat, Cambridge University Press, Cambridge, 2009.
[19] M. Dolder, K. Zeth, P. Tittmann, H. Gross, W. Welte, T. Wallimann, Crystallization of the human, mitochondrial voltage-dependent anion-selective channel in the presence of phospholipids, J. Struct. Biol. 127 (1999) 64–71, https://doi.org/10.1006/jsbi.1999.4141.
[20] M.T. Eddy, T.C. Ong, L. Clark, O. Teijido, P.C. van der Wel, R. Garces, G. Wagner, T.K. Rostovtseva, R.G. Griffin, Lipid dynamics and protein-lipid interactions in 2D crystals formed with the beta-barrel integral membrane protein VDAC1, J. Am. Chem. Soc. 134 (2012) 6375–6387, https://doi.org/10.1021/ja300347v.
[21] U. Zachariae, R. Schneider, R. Briones, Z. Gattin, J.P. Demers, K. Giller, E. Maier, M. Zweckstetter, C. Griesinger, S. Becker, R. Benz, B.L. de Groot, A. Lange, beta-Barrel mobility underlies closure of the voltage-dependent anion channel, Structure 20 (2012) 1540–1549, https://doi.org/10.1016/j.str.2012.06.015.
[22] E.E. Najbauer, K.T. Movellan, T. Schubeis, T. Schwarzer, K. Castiglione, K. Giller, G. Pintacuda, S. Becker, L.B. Andreas, Probing membrane protein insertion into lipid bilayers by solid-state NMR, ChemPhysChem 20 (2019) 302–310, https://doi.org/10.1002/cphc.201800793.
[23] V.Y. Orekhov, V.A. Jaravine, Analysis of non-uniformly sampled spectra with multi-dimensional decomposition, Prog. Nucl. Magn. Reson. Spectrosc. 59 (2011) 271–292, https://doi.org/10.1016/j.pnmrs.2011.02.002.